RSC Advances

PAPER

View Article Online
View Journal | View Issue

Cite this: *RSC Adv.*, 2017, 7, 52352

Effect of high concentration SO_2 on four-way catalytic performance of $La_{0.9}Sr_{0.1}Pd_{0.03}Mn_{0.97}O_3$ perovskite catalysts

Li Yang,[a] Guobin Li,[a] Gewu Gao,[a] Ruile Xu,[a] Shuwei Zhu,[a] Xinqian Shu,*[a] Sujian Wang,[b] Zengshe Deng[b] and Peng Wang[b]

Received 10th August 2017
Accepted 30th October 2017

DOI: 10.1039/c7ra08833g

rsc.li/rsc-advances

The influence mechanism of SO_2 on the NO_x removal performance of a $La_{0.9}Sr_{0.1}Mn_{0.97}Pd_{0.03}O_3$ catalyst was investigated in this paper using X-ray diffraction, scanning electron microscopy, Fourier transform infrared spectroscopy, and the transient response method. Results show that incorporating the noble metal Pd into the catalyst increases the specific surface area of the original catalyst, creating a suitable place for NO_x contact, reducing the ignition temperature of soot and improving the NO_x, C_3H_6 and CO conversion of the catalyst effectively. Although the catalyst $La_{0.9}Sr_{0.1}Mn_{0.97}Pd_{0.03}O_3$ forms a stable and irreversible sulphate after reacting in a high concentration of SO_2 (300 ppm) atmosphere, it retains a high removal efficiency of NO_x.

1. Introduction

The rapid development of the national economy has led to serious environmental pollution. Environmental pollution can be attributed to the rapid development of the transportation industry and the continuous increase of vehicle ownership. In a diesel engine exhaust, NO_x is the main reason for the formation of acid rain, as well as in the atmosphere with the photochemical reaction of hydrocarbons, generating ozone and other highly oxidizing substances that lead to photochemical smog. NO_x is the main source of an irritating odor, which seriously affects human health. The emissions of soot particles can cause numerous respiratory diseases and seriously harm human health. Therefore, countries around the world are working to develop new technologies for tail gas treatment to address the problems of environmental pollution caused by diesel engine soot particles and NO_x emissions. Since fuels contain residual sulphur, the problem of SO_2 poisoning also has become one of the main issues in the development of technologies in NO_x elimination.[1,2] Particularly, with the increasingly extensive use of diesel vehicles, efficiently processing diesel exhaust is not only an important issue but is also the future policy trend. The simultaneous treatment of four pollutants in diesel exhaust (four-way catalytic technology) has become progressively urgent.

Perovskite-type compounds have numerous advantages, such as oxygen vacancy and good thermal conductivity, as well as B-valence ions, which have the advantages of the mixed and abnormal valence states while maintaining the structure. In addition, perovskite-type compounds have a certain conversion capacity of NO under lean-burn conditions. Therefore, the perovskite-type material is expected to become the new generation of automotive exhaust gas purification catalyst.[3]

At present, four-way combination catalysis has numerous problems, such as high running cost, complicated structure, and substantially occupied space. For example, the catalyst used for soot-NO_x oxidation and reduction has low NO_x conversion rate, poor selectivity, sulfur poisoning, and other issues.[4–6]

Mn has a variable d electronic structure and a variety of valence state, which shows good redox properties. La has a large atomic radius and high thermal stability. Therefore, $LaMnO_3$ is a high-temperature stable redox catalyst that has been applied in numerous fields, such as fuel cells, gas sensors, magnetic structures, hydrocarbon oxidation combustion, and so on.[7–12] The Mn^{4+} and oxygen vacancies appear in the $La_{1-x}Sr_xMnO_3$ system after doping Sr^{2+} ions at the A-site of $LaMnO_3$. Therefore, the metal oxide catalyst of perovskite-type composite has excellent catalytic activity. The results show that the addition of a small amount of noble metal in the perovskite catalyst can improve the catalytic activity of the sample. The perovskite-type oxide catalyst with a small amount of noble metal Pd has higher catalytic activity even in high-temperature water vapor, as well as sulfide exhaust, which can also possess high catalytic performance for a long period of time.[13–15] Our ($La_{1-x}Sr_xMn_{1-y}Pd_yO_3$) catalyst has simultaneously excellent redox properties with the alkaline storage centers Sr and catalytically active centers Pd, thereby creating a promising four-way catalyst.

---

[a] *School of Chemical & Environmental Engineering, China University of Mining & Technology, Beijing 100083, China. E-mail: sxq@cumtb.edu.cn; Fax: +86-01062331853; Tel: +86-01062331853*

[b] *Shaanxi Coal and Chemical Industry Group Company, Xi'an, 710065, China*

2. Experimental methods

2.1 Preparation

The $La_{1-x}Sr_xMn_{1-y}Pd_yO_3$ materials with the intended atomic ratios of 0.9/0.1/0.97/0.03 were synthesized by co-precipitation method. Citric acid (25.2 g) dissolved in the deionized water according to the molar ratio (citric acid : the sum of metal ions = 1.2 : 1). The two solutions were mixed together and stirred for 10 h under reflux to obtain the wet gel. Then, the mixture was dried overnight in a vacuum oven at 120 °C to sublimate the water. The dry gel was transferred into the crucible after being crushed and grinded. A subsequent calcination of the translucent residue is made at 200 °C for 4 h, and then calcined at 700 °C for 6 h.

2.2 Characterization

Scanning electron microscopy (SEM; Hitachi, Japan) with a 15 kV accelerating voltage and 100–5000 times amplification factor was used to analyze the surface of the adsorbent in the experiment. X-ray diffraction (XRD) was used to discuss the form of adsorbent (Ultima, Japan, Cu Kα radiation, power 40 kV × 40 mA). Nitrogen adsorption–desorption isotherm method (NOVA4000, Quantachrome) was used to test the specific surface area. Fourier transform infrared spectroscopy (FTIR; Magna-IR750, Nicolet) was used to analyze the surface functional groups of the catalyst.

Temperature programmed reaction was conducted with a GSVH of 20 000 h^{-1}. The catalysts were directly exposed to reaction gas containing NO (0.1%), C_3H_6 (0.05%), CO (0.5%), O_2 (10%) and SO_2 (300 ppm). The composition of the gas mixture produced from the reaction was analyzed by the online A5000 model gas chromatograph.

The ignition temperature of soot (T_{ig}) and the conversion rate of polluted gas (X_{NO}, X_{CO}, $X_{C_3H_6}$) were used as the evaluation index of the activity of the catalyst. In the reaction process, the conversion rate of the reaction gas is calculated by the following formula:

$$X_{NO} = \frac{[NO]_i - [NO]_O}{[NO]_i} \times 100\% \qquad (1)$$

$$X_{CO} = \frac{[CO]_i - [CO]_O}{[CO]_i} \times 100\% \qquad (2)$$

$$X_{C_3H_6} = \frac{[C_3H_6]_i - [C_3H_6]_O}{[C_3H_6]_i} \times 100\% \qquad (3)$$

thereinto: X: represents conversion rate i: inlet concentration, O: export concentration.

3. Results and discussion

3.1 Catalysts characterization

Fig. 1 shows the comparison between the XRD map of $La_{0.9}Sr_{0.1}MnO_3$ and $La_{0.9}Sr_{0.1}Mn_{0.97}Pd_{0.03}O_3$ catalysts. As seen from the figure, the peak intensity slightly decreased but still maintained a good perovskite structure after Pd doping. The mean crystallite size (dp) of supports, the perovskite and the supported perovskites were calculated from the line broadening of the most intense reflections using the Debye–Scherrer equation.

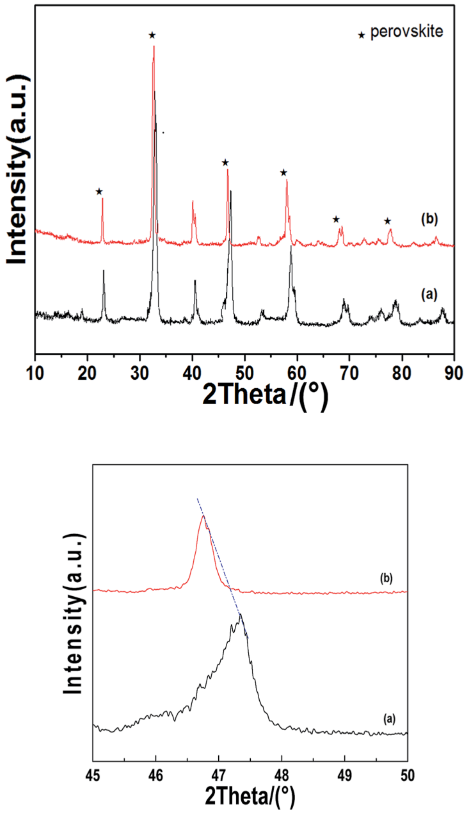

Fig. 1 XRD of the catalyst and its amplification (right) map (a) $La_{0.9}Sr_{0.1}MnO_3$; (b) $La_{0.9}Sr_{0.1}Mn_{0.97}Pd_{0.03}O_3$.

$$dp = \frac{k \times \lambda}{B_{1/2} \times \cos\theta} \qquad (4)$$

where $B_{1/2}$: the line broadening at half the maximum intensity (FWHM) in radians, λ: wavelength, cos θ: Bragg angle, dp: the mean size of the ordered (crystalline) domains, which may be smaller or equal to the grain size.

Doping Pd to the perovskite structure shifted the diffraction peaks to a small angle. When the Mn^{4+} is replaced by Pd^{2+}, the size of the perovskite cell increased and the diffraction peak position shifted to a small angle because the ionic radius of Pd^{2+} (0.64 Å) is larger than Mn^{4+}(0.39 Å). The change of unit cell parameters before and after doping is shown in Table 1. After

Table 1 Crystal structures, lattice parameters and specific surface area of catalysts

	Cell parameters (Å)				
Composition	*a*	*b*	*c*	*d*	BET (m^2 g^{-1})
$La_{0.9}Sr_{0.1}MnO_3$	5.48	3.83	9.84	109	8.72
$La_{0.9}Sr_{0.1}Pd_{0.97}Mn_{0.03}O_3$	5.55	5.43	10.12	164	11.04

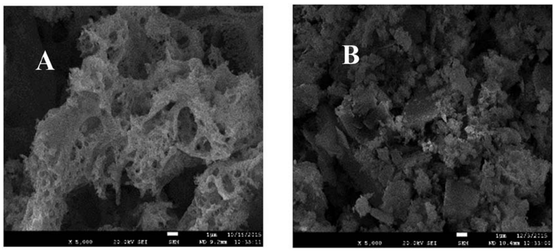

Fig. 2 SEM photos of $La_{0.9}Sr_{0.1}MnO_3$ and $La_{0.9}Sr_{0.1}Mn_{0.97}Pd_{0.03}O_3$ catalysts.

doping, the lattice parameters *a*, *b* and *c* of the crystallite increase and the specific surface area is increased from 8.72 $m^2\ g^{-1}$ to 11.04 $m^2\ g^{-1}$, which may be related to the distortion of the crystal.[16]

Fig. 2A and B are SEM photographs of $La_{0.9}Sr_{0.1}MnO_3$ and $La_{0.9}Sr_{0.1}Mn_{0.97}Pd_{0.03}O_3$, respectively, catalyst magnified 5000 times.

The figure shows that the $La_{0.9}Sr_{0.1}MnO_3$ catalyst particles are stacked together like a structure of flocculent, which may be attributed to insufficient uniform dispersion. The scale of $La_{0.9}Sr_{0.1}Mn_{0.97}Pd_{0.03}O_3$ catalyst particles doped with Pd became significantly smaller and the particle size distribution is uniform. Due to the high temperature calcination, the surface of the sample is sintered and some of the channels collapsed together, resulting in a lot of irregular voids. The formation of the pore became abundant, which is conducive to increasing the surface area of the catalyst and further promoting the contact and adsorption effect with pollutants. The conclusion is consistent with the results of the specific surface area been shown in Table 1.

3.2 Comparison of $La_{0.9}Sr_{0.1}MnO_3$ catalytic activity before and after doping pd

Fig. 3 shows the conversion ratio of CO, C_3H_6 and NO before and after doping of the $La_{0.9}Sr_{0.1}MnO_3$ catalyst with noble metal Pd. The results showed that the removal efficiency of CO, C_3H_6 and NO of doping (b) is significantly higher than that of undoped (a). The average conversion rate of CO over $La_{0.9}Sr_{0.1}MnO_3$ was only 23.69%; however, the conversion rate of CO was gradually increased with the increase of the temperature of the doped $La_{0.9}Sr_{0.1}Mn_{0.97}Pd_{0.03}O_3$ catalyst, reaching 50% at 360 °C. The average conversion rate of NO over $La_{0.9}Sr_{0.1}MnO_3$ was 63.81%, whereas that of $La_{0.9}Sr_{0.1}Mn_{0.97}Pd_{0.03}O_3$ was 92.25%. The average conversion rate of propene over $La_{0.9}Sr_{0.1}MnO_3$ and $La_{0.9}Sr_{0.1}Mn_{0.97}Pd_{0.03}O_3$ was 60.17% and 73.68%, respectively. Indicating that the element of palladium promotes the oxidation of propene effectively. Additionally, the temperature of soot combustion over catalysts of $La_{0.9}Sr_{0.1}MnO_3$ and $La_{0.9}Sr_{0.1}Mn_{0.97}Pd_{0.03}O_3$ was 354 °C and 257 °C, respectively. After doping Pd, the valence state of Pd^{2+} is lower than Mn^{3+}. A substantial number of oxygen vacancies or high valence Mn^{4+} ions appear to maintain the charge balance. Increasing the oxygen vacancies and the mobility of oxygen is beneficial to the oxidation of NO_2 to NO in the form of nitrate in SrO and $SrCO_3$. With the appropriate temperature point between NO_x desorption and reducing gas, CO reacted and thus also improved the CO conversion rate and the reaction process is as follows.

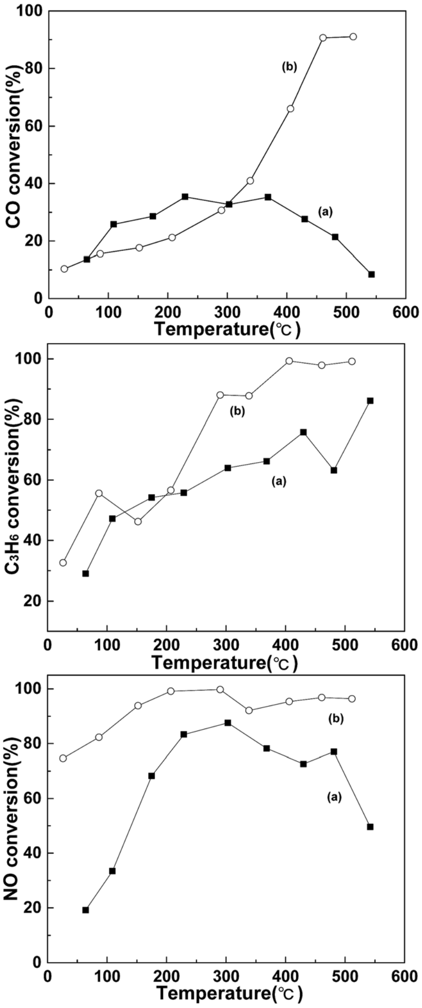

Fig. 3 Comparison of CO, C_3H_6 and NO conversion before and after Pd doping (a) $La_{0.9}Sr_{0.1}MnO_3$; (b) $La_{0.9}Sr_{0.1}Mn_{0.97}Pd_{0.03}O_3$.

$$\text{Pd–NO} + \text{Pd–O} \rightarrow \text{Pd–NO}_2 + \text{Pd} \tag{5}$$

$$SrCO_3 + 2NO_3 \rightarrow Sr(NO_3)_2 + CO_2 + O^{2-} \tag{6}$$

$$SrO + 2NO_3 \rightarrow Sr(NO_3)_2 + O^{2-} \tag{7}$$

In summary, the doping of noble metal Pd can effectively improve the performance of the catalyst activation.

4. Effect of SO_2 on the removal efficiency of $La_{0.9}Sr_{0.1}Mn_{0.97}Pd_{0.03}O_3$

4.1 Catalyst characterization

Fig. 4 shows the XRD patterns of the $La_{0.9}Sr_{0.1}Mn_{0.97}Pd_{0.03}O_3$ catalyst in the high concentration SO_2 condition before and

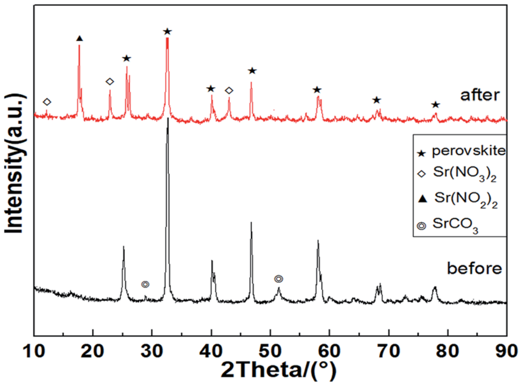

Fig. 4 XRD pattern of the catalyst before and after sulfur test.

after the mixed gas test. The figure shows that after prolonged reaction of catalysts under high SO_2 concentration, the diffraction peak in the perovskite strength remained unchanged, thereby indicating the effect of a high concentration of SO_2 on the perovskite structure in the sample is not large and the structure remained relatively good and stable. In addition, sulfate diffraction peaks were absent in the spectra of the reaction, which shows that the samples did not obviously form sulfate particles after the durability test under high concentration SO_2. However, it can't exclude that a small amount of sulfate species highly dispersed on the sample surface. X-ray diffraction analysis showed that the diffraction peaks of $SrCO_3$ in fresh catalyst became weak after mixed gas test while the nitrate $Sr(NO_3)_2$ and $Sr(NO_2)_2$ diffraction peaks were observed, indicating that the $SrCO_3$ is the storage sites of NO_x and the catalyst has a strong sulfur-resistance performance.

Fig. 5 shows the results of the mixture experiment FTIR over $La_{0.9}Sr_{0.1}Mn_{0.97}Pd_{0.03}O_3$ catalyst. Fig. 5 also shows spectral patterns exhibiting peaks at approximately 1624 cm^{-1}, which are assigned to the deformation vibration and stretching vibration of O–H bonds of the adsorbed water. 848 cm^{-1} and 1468 cm^{-1} correspond to the characteristic peak of carbonate. In addition, after SO_2-containing gases test the minor absorption associated with nitrate species (broad at 1396 cm^{-1} due to ionic nitrates) and ionic nitrites (1207 cm^{-1}) are evident. This minor absorption can be attributed to the formation of nitrates by NO_x adsorbed on the carbonate surface, which corresponds to the transformation from strontium carbonate to strontium nitrate. The characteristic peaks of carbonates disappeared after the SO_2-containing gases test and the free ionic nitrates appeared, thereby indicating that the NO_x was stored on the carbonate of the catalyst surface. 1128 cm^{-1} is the characteristic peak of the bulk sulfate species, and the samples after SO_2-containing gases test showed a weak vibration peak of sulfate. The absorption peak at 621 cm^{-1} is the characteristic vibration peak of the perovskite structure. The results show that the perovskite structure of the prepared catalyst is well, and the structure of the sample remained well after the mixed gas experiment. This indicates that SO_2 has a slight effect on the structure of the catalyst, which is similarly to the previous XRD results.

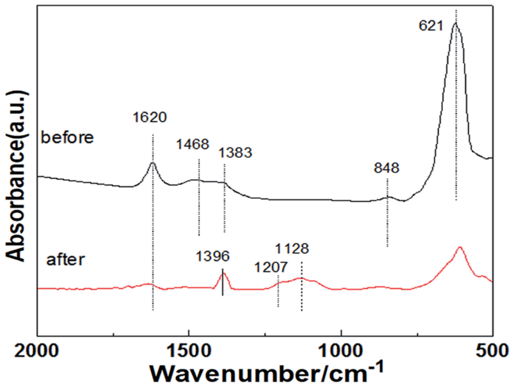

Fig. 5 FTIR pattern of the catalyst before and after sulfur test.

4.2 Catalytic test: sulfur tolerance

The temperature program reactions of supported perovskites were evaluated in a fixed bed.

Fig. 6 displays the corresponding conversion-temperature profiles of the $La_{0.9}Sr_{0.1}Mn_{0.97}Pd_{0.03}O_3$ catalyst during the SO_2-containing gases and non-SO_2 gases test. The figure reveals that the with the increase of T, the conversion rate of NO at the low temperature range (100–200 °C) is increased and the yield of NO_2 is correspondingly increased, but the yield of N_2 does not change too much. The results indicating that the oxidation of NO to NO_2 occurs mainly at low temperature range and NO_2 stored in the catalyst in the form of nitrate, corresponding to the previous FT-IR results. When the temperature continues rise, the yield of NO_2 decreased while the N_2 begin to increase, indicating that the NO_x reduced to N_2 by reducing gas (CO, C_3H_6). Meanwhile it can be seen that SO_2 has little effect on the oxidation reaction of NO–NO_2, but it has some influence on the reduction of NO_x during the mixture gas test. A competitive adsorption of the SO_2 and NO_x on the surface of the catalysts occurs which may probably be due to the NO_2 storage stage. The sulfate is more stable than the nitrate and the SO_2 is occupied by the mixed gas atmosphere containing SO_2 because the (p–d) π bond in the sulfate structure is more stable than the delocalized π-bond in the nitrate, resulting in a decrease in the

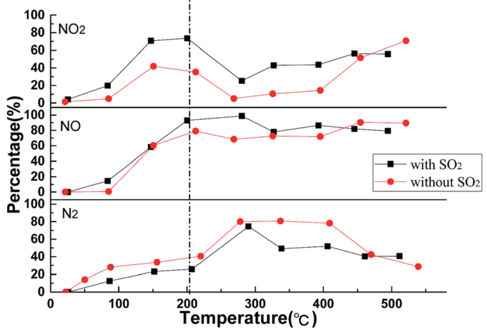

Fig. 6 Effect of sulfur on the NO conversion as well as NO and N_2 yields of the catalyst.

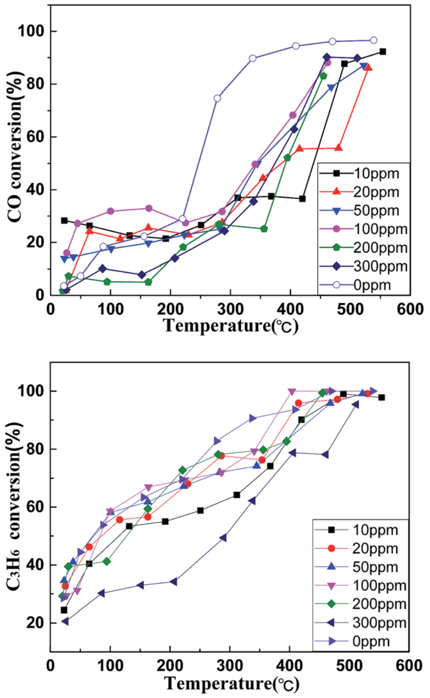

Fig. 7 Effect of different sulfur concentrations on the CO and C_3H_6 conversion of the catalyst.

storage capacity of the catalyst for NO_x. The result affects the effective progress of the catalyst reduction reaction.

Fig. 7 illustrates different effects of SO_2 concentration on the N_2 yield and the CO removal rates of the catalyst ($La_{0.9}Sr_{0.1}Mn_{0.97}Pd_{0.03}O_3$), respectively. The figures show the catalyst $La_{0.9}Sr_{0.1}Mn_{0.97}Pd_{0.03}O_3$ has a high catalytic activity without the presence of SO_2, 303 °C, the removal rate of CO which has reached more than 80%, the yields of N_2 were up to 87%. When the SO_2 concentration is lower than 200 ppm, the denitration efficiency of the catalyst has a slight effect. When SO_2 concentrations are up to 300 ppm, the catalytic activity significantly decreased. At a temperature of 303 °C, the highest removal rate of CO is only 27%, and the highest conversion rate of C_3H_6 is 78%. In addition, the soot ignition temperature is 368 °C, which is 15% higher than that of non-SO_2 312 °C, indicating that the catalyst possesses some resistance on low concentrations of SO_2. SO_2 with high concentrations will obviously inhibit the catalytic activity of $La_{0.9}Sr_{0.1}Mn_{0.97}Pd_{0.03}O_3$. When the concentration of sulfur is higher, the storage capacity of NO_x is lower, resulting in catalyst poisoning.

5. Conclusions

After doping with noble metal Pd, the conversion rate of CO and NO obviously increased. This catalytic activity increase can be attributed to the increased oxygen vacancies and the oxygen mobility after the doping of Pd. FT-IR analyses showed that NO_x was stored in the catalyst and the $La_{0.9}Sr_{0.1}Mn_{0.97}Pd_{0.03}O_3$ catalyst has a certain tolerance to SO_2. These results indicate that high NO_x removal efficiency can be achieved by doping pd in perovskites of $La_{0.9}Sr_{0.1}MnO_3$.

Conflicts of interest

There are no conflicts to declare.

Acknowledgements

The project is financially supported by the National Natural Science Foundation of China (51074170.).

References

1 E. Chaize, D. Webster, B. Krutzsch, G. Wenninger, M. Weibel, S. Hodjati, C. Petit, V. Pitchon, A. Kiennemann, R. Loenders, O. Monticelli, P. A. Jacobs, J. A. Martens and J. A. B. Kasemo, *SAE 982593*, Society of Automotive Engineers, 1998.
2 S. Hodjati, C. Petit, V. Pitchon and A. Kiennemann, Absorption/desorption of NOx process on perovskites: impact of SO2 on the storage capacity of BaSnO3 and strategy to develop thioresistance, *Appl. Catal., B*, 2000, **30**, 247–257.
3 Y. Liu and Y. N. Qing, *J. Nat. Gas Chem.*, 1997, **22**(6), 47–51.
4 P. Denton, A. Giroir-Fendler, H. Praliaud, *et al.*, Role of the rlature of the support (alumina or silica), of the support porosity, and of the Pt dispersion in the selective reduction of NO by C_3H_6 under lean-bum condition, *J. Catal.*, 2000, **189**(2), 410–420.
5 Y. Shougeng, Advance in after treatment technology for diesel vehicle's Exhaust Gas, *Precious Met.*, 2003, **24**(1), 62–66.
6 S. J. Park, H. A. Ahn, I. J. Heo, I.-S. Nam, J. H. Lee, Y. K. Youn and H. J. Kim, Hydrotalcite as a Support for NOx Trap Catalyst, *Top. Catal.*, 2010, **53**, 57–63.
7 F. Yang, S. Kim, Y. Takamura, *et al.*, *Scr. Mater.*, 2011, **65**(1), 29–32.
8 S. Cimino, L. Lisi, R. Pirone, *et al.*, *Catal. Today*, 2000, **59**(1–2), 19–31.
9 E. N. Armstrong, T. Striker, V. Ramaswamy, *et al.*, *Sens. Actuators, B*, 2011, **158**(1), 159–170.
10 M. Alifanti, J. Kirchnerova, B. Delmon, *et al.*, *Appl. Catal., A*, 2003, **245**(2), 231–244.
11 Z. J. Sui, L. Vradman, I. Reizner, *et al.*, *Catal. Commun.*, 2011, **12**(15), 1437–1441.
12 E. A. Parvaneh, K. Abbasali, Z. A. Hessam, *et al.*, *Chem. Eng. J.*, 2011, **169**, 282–289.
13 H. Tanaka, H. Fujikawa and I. Takahashi, Perovskite-Pd three-way catalysts for automotive applications, *SAE paper 930251*, 1993.
14 H. Tanaka and I. Takahashi, Advances in designing perovskite catalysts, *SAE J.*, 1993, **47**(10), 51.
15 H. Tanaka, H. Fujikawa and I. Takahashi, Excellent oxygen storage capacity of perovskite-PD three-way catalysts, *SAE paper 950256*, 1995.
16 L. Zhu, X. Wang and C. Liang, Catalytic combustion of diesel soot over K_2NiF_4-type oxides $La_{2-x}KxCuO_4$, *J. Rare Earths*, 2008, **2**, 254–257.